X-ray reflectivity and atomic force microscopy studies of MOCVD grown $Al_xGa_{1-x}N$/GaN superlattice structures*

Wang Yuanzhang(王元樟)[1,2,†], Li Jinchai(李金钗)[2], Li Shuping(李书平)[2], Chen Hangyang(陈航洋)[2], Liu Dayi(刘达艺)[2], and Kang Junyong(康俊勇)[2]

[1]Department of Mathematics and Physics, Xiamen University of Technology, Xiamen 361024, China
[2]Fujian Key Laboratory of Semiconductor Materials and Applications, Xiamen University, Xiamen 361005, China

Abstract: The grazing incidence X-ray reflectivity (GIXR) technique and atomic force microscopy (AFM) were exploited to obtain an accurate evaluation of the surfaces and interfaces for metalorganic chemical vapor deposition grown $Al_xGa_{1-x}N$/GaN superlattice structures. The X-ray diffraction results have been combined with reflectivity data to evaluate the layer thickness and Al mole fraction in the AlGaN layer. The presence of a smooth interface is responsible for the observation of intensity oscillation in GIXR, which is well correlated to step flow observation in AFM images of the surface. The structure with a low Al mole fraction ($x = 0.25$) and thin well width has a rather smooth surface for the R_{rms} of AFM data value is 0.45 nm.

Key words: metalorganic chemical vapor deposition; interfaces; surfaces; nitrides; superlattices; high resolution X-ray diffraction

DOI: 10.1088/1674-4926/32/4/043006 **EEACC:** 2520

1. Introduction

The wide-bandgap III nitride semiconductors have attracted much attention for their optoelectronic applications. Among these compounds, $Al_xGa_{1-x}N$/GaN heterostructures have been the subject of intensive investigation, because their large band offset and large polarization effect make them suitable for applications in high voltage and high power microwave devices, such as high-electron-mobility transistors (HEMT)[1] and field-effect transistors (FET)[2−9]. The AlGaN layer thickness, composition and strain are significant parameters in the AlGaN/GaN HEMT structure, which determine the two-dimensional electron gas (2DEG) sheet charge density in the channel resulting from piezoelectric and spontaneous polarization. Hence, the accurate determination of these parameters is very important.

Compared with the AlN/GaN heterostructures grown by molecular beam epitaxy (MBE)[10], it seems that those grown by metalorganic chemical vapor deposition (MOCVD) have a problem in achieving abrupt and flat heterointerfaces. This might be due to the higher substrate temperatures in MOCVD and the three-dimensional growth of AlN on GaN. An abruptness and a flatness of heterointerface are very important parameters to achieve high performance in the above devices. As a quantitative method for characterizing the abruptness of a heterointerface, grazing incidence X-ray reflectivity (GIXR) was proved to be effective to estimate structural features in heteroepitaxial layers[11]. When applied to a smooth AlGaN/GaN superlattice (SL), GIXR can provide detail about not only the thickness of the individual layers in a multilayer periodicity but also the root-mean square (RMS) roughness on the interfaces and surface. In conjunction with X-ray reflectivity, X-ray diffraction (XRD) is employed to obtain epi-layer crystallinity, layer thickness and composition[12]. Cross related to X-ray reflectivity techniques is atomic force microscopy (AFM) surface morphology for the evaluation of epi-layer quality. While the GIXR is able to obtain information at small length scales, AFM images can reveal the presence of large vertical features that tend to mask the surface characteristics at nanometer length scales. In addition to surface roughness, the presence of step flow growth can readily be assessed by AFM. In this study, surface roughness measurements were performed with these two techniques to accurately characterize the surface of $Al_xGa_{1-x}N$/GaN SL grown by MOCVD.

2. Experiment

The samples of six-period $Al_xGa_{1-x}N$/GaN SL were grown by low-temperature MOCVD in a vertical reactor (Thomas Swan 3x2″ CCS) on (0001) sapphire substrates using TMGa and NH_3 as precursors and H_2/N_2 as a carrier gas. An *in situ* interferometer setup was used to monitor the growth procedures. Reflectance was detected using a semiconductor laser operating at a wavelength of 635 nm, which points at the sample surface through a quartz probe fed through the showerhead of the reactor. Reflectance was recorded and normalized to the reflectivity of the bare sapphire substrate. After depositing a low-temperature GaN nucleation layer, a 2 μm-thick undoped GaN buffer layer was grown at about 1030 ℃. Then a six-period $Al_xGa_{1-x}N$/GaN SL was grown on the undoped GaN at 1040 ℃, under pressure of 70 Torr. Five samples were grown, in which the barrier width is about 10 nm, while the Al mole fraction varies from 0.25 to 0.45 and the well width varies from 4 to 7 nm. A high-resolution X-ray diffraction sys-

* Project supported by the National Natural Science Foundation of China (No. 60876008) and the Science and Technology Program of the Educational Office of Fujian Province, China (No. JA10249).
† Corresponding author. Email: yzhwang@xmut.edu.cn
Received 14 September 2010, revised manuscript received 18 November 2010
© 2011 Chinese Institute of Electronics

Table 1. Well width, barrier width, composition of AlGaN layer, FWHM of XRDCRC and surface roughness by GIXR and AFM for samples A, B, C, D and E.

Sample No.	Well width (nm)	Barrier width (nm)	Al mole fraction	XRDCRC FWHM (arcsec)	R_{rms} by GIXR (nm)	R^*_{rms} by AFM (nm)	R_{am} by AFM (nm)
A	4.0	10.6	0.25	217	0.50	0.45	0.30
B	5.9	10.6	0.25	210	0.78	0.88	0.54
C	6.8	10.6	0.25	230	0.98	1.03	0.70
D	4.0	10.6	0.35	250	0.55	0.66	0.46
E	4.0	10.6	0.45	202	1.20	1.70	0.85

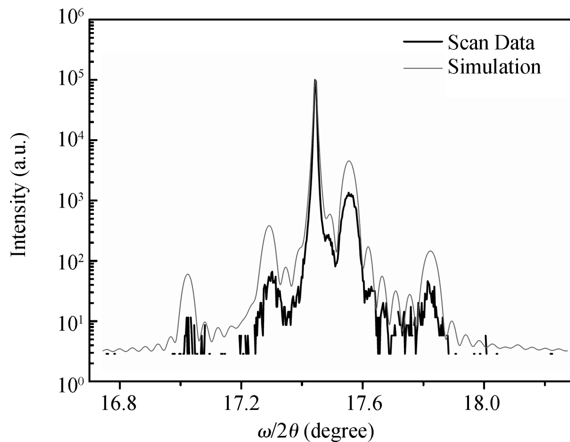

Fig. 1. X-ray diffraction profile of sample A. Clear fringes due to the AlGaN layer were observed.

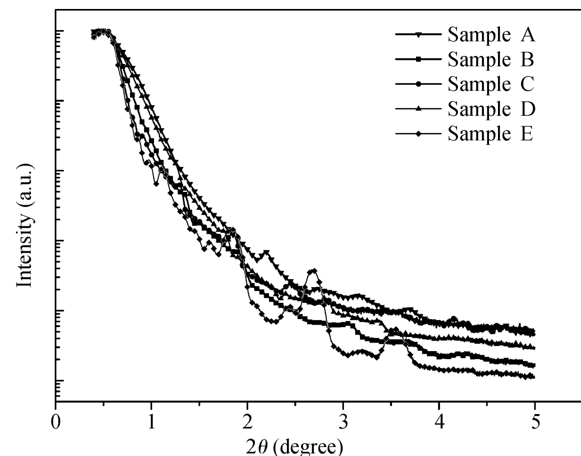

Fig. 2. GIXR spectra of samples A, B, C, D and E.

tem (Philips MRD) with a four-crystal Bartel monochrometer and CuKα1 line at 1.54056 Å was used to determine the barrier and well width as well as the Al mole fractions. Philips software based on the Takagi–Taupin model[13,14] was used for diffraction profile simulation. The GIXR was measured by a 2θ–ω scan from 0.4° to 5.0°. For GIXR simulations, we used a fitting based on the theories of Parrat[15] and Nevot–Croce[16]. The surfaces of the samples were observed by AFM (SII Nano Technology Inc.) using dynamic force mode. The size of the area measured by AFM is significant in relation to the RMS roughness value that it produces. A 1×1 μm^2 area is often relatively flat and is not an accurate representation of the surface, while a 5×5 μm^2 area represents the surface much better. We use such an area for quantifying the surface roughness. To obtain reliable AFM images as well as surface roughness data, at least five regions of each sample were examined. The root mean square deviation R^*_{rms} and arithmetic mean deviation R_{am} of AFM data values for a given area were used to describe the surface roughness of the samples.

3. Results and discussion

The high-resolution X-ray diffraction profiles of five samples were exploited to accurately evaluate thickness, Al mole fraction, and crystallinity. These are listed in Table 1. Since the well and barrier layer are thin, they remain pseudomorphic and almost fully strained. This allows determination of the Al mole fraction, assuming Vegard's rule of linearity of lattice constant with composition for a ternary compound. The Poisson ratio values used in our calculations were evaluated by Wright[17]. The GaN buffer layers were measured to be fully relaxed and the full width at half maximum (FWHM) of the (0002) reflection X-ray double-crystal rocking curve profiles are within 200–250 arcsec. These high values of GaN FWHM are attributed to the mosaic spread existing in the GaN films, which can be evaluated and separated from the residual strain by triple axis high resolution XRD measurements. Figure 1 shows the triple axis XRD profile and simulated curve of sample A. The FWHM is only 31 arcsec for the GaN line. Clear fringes due to the AlGaN layer were also observed, indicating a relatively smooth and abrupt AlGaN/GaN heterointerface and high structural quality of the epi growth.

The results of GIXR are shown in Fig. 2. The intensity oscillations due to the AlGaN layer are clearly visible in these profiles, indicating rather smooth surfaces and interfaces. Especially in the profile of sample E, remarkable oscillation can be observed which is due to the high Al mole fraction. On the other hand, as shown in Fig. 2, the X-ray reflectivity intensity slowly decreased for samples A and D compared to samples B, C and E. This suggests that the surface and the interface roughnesses of samples A and D are more abrupt than samples B, C and E, which is consistent with the surface roughness measured by AFM, as shown in Table 1. The simulated surface roughnesses R_{rms} of these five sample profiles are also listed in Table 1. The composition and thickness of the AlGaN layers in the simulation were confirmed by XRD radial scanning along (0002). The roughness, thickness and density of the individual layers were estimated from the fitting of the GIXR simulation profile. Here, in Table 2 the description and parameters of sample A are tabulated. The interfaces are rather smooth for the roughnesses are only around 3 Å. The average thick-

Table 2. Description and parameters for six-period GaN/$Al_xGa_{1-x}N$ SL structure (sample A).

Layer	Roughness, σ_j (Å)	Thickness , d_i (Å)	Density (g/cm^{-3})
(1) GaN	5.0	45.7	3.871
(2) $Al_{0.25}Ga_{0.75}N$	3.6	101.2	5.882
(3) GaN	3.2	43.0	5.930
(4) $Al_{0.25}Ga_{0.75}N$	2.9	109.9	5.862
(5) GaN	2.8	42.3	5.910
(6) $Al_{0.25}Ga_{0.75}N$	2.6	110.0	5.877
(7) GaN	2.6	35.3	5.931
(8) $Al_{0.25}Ga_{0.75}N$	2.5	110.3	5.908
(9) GaN	2.3	41.0	5.995
(10) $Al_{0.25}Ga_{0.75}N$	2.2	103.6	5.895
(11) GaN	2.0	44.7	5.960
(12) $Al_{0.25}Ga_{0.75}N$	1.7	114.2	5.882

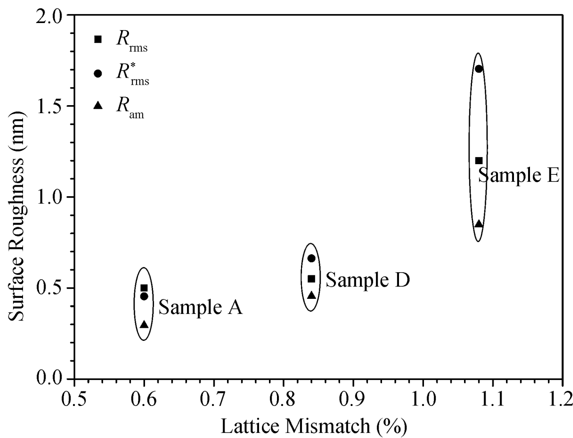

Fig. 3. Relationship between surface roughness and lattice mismatch. Sample A ($x = 0.25$), D ($x = 0.35$) and E ($x = 0.45$) have the same well and barrier widths.

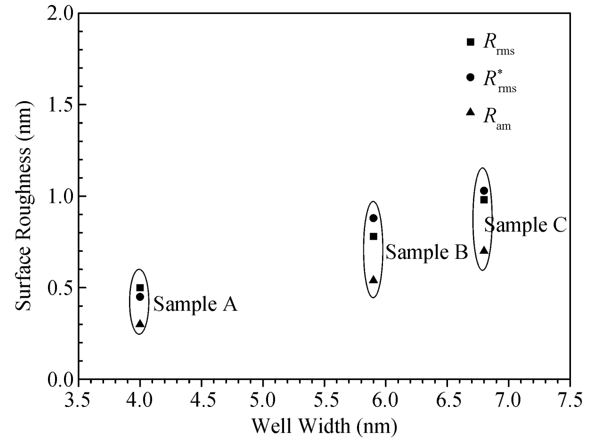

Fig. 4. Relationship between surface roughness and well width. Samples A, B and C have the same $Al_{0.25}Ga_{0.75}N$ barrier width (10.6 nm).

nesses of GaN and AlGaN are very close to the results of high-resolution M-ray diffraction. The density of the individual layers indicated the existence of strain. They are all compressed due to the thermal strain which is originated from the difference of thermal expansion coefficients between epi-layers and substrates during cooling from the growth temperature to room temperature. The layer (1) was part oxidized, which has been confirmed by auger electronic spectrum (AES), so it has much lower density than other epi-layers.

While GIXR affords macroscopic measurement of surface roughness, AFM evaluates microscopic scale roughness. The AFM roughness values R^*_{rms} and R_{am} given by a 5 × 5 μm^2 area are also listed in Table 1. The results show that the surface roughnesses by GIXR agree with the data estimated by AFM, indicating that GIXR is effective in estimating the structural properties of AlGaN/GaN heterostructures. Figure 3 shows the relationship between surface roughness and the lattice mismatch. For comparison, the chosen samples have the same well and barrier widths but different lattice mismatch (Al mole fraction $x = 0.25, 0.35, 0.45$). The surface roughness R^*_{rms} increased from 0.45 to1.7 nm, as the lattice mismatch increased from 0.60% to 1.08%. The sample E with a high lattice mismatch has a much rougher surface. This might be due to the lattice mismatch increase in the AlGaN/GaN heterostructure with high Al composition, which causes the three-dimensional growth of AlGaN on GaN. Figure 4 shows the relationship between the surface roughness and the well width. Samples A, B, and C have the same $Al_{0.25}Ga_{0.75}N$ barrier width. The surface roughness increased with increasing well width. As the AlGaN/GaN heterostructure grows, the elastic strain energy increases and is accommodated by the lattice. Since the sample with the thicker well width has a higher elastic strain energy, the more dislocation may produce for releasing the energy, and make the surface rougher. All of the above indicate that the stress which comes from lattice mismatch in the AlGaN/GaN heterostructure is the main cause of interface and surface roughness.

Figure 5 shows an AFM image of sample A. Here for clarity we present the 3 × 3 μm^2 area figure. A step-like flat surface has also been observed. The lateral step sizes are of the order of 100 nm in most samples except the high Al composition one. This dimension appears to be significant, since samples with a smaller step size also have rougher surfaces and samples with larger than 100 nm have smoother surfaces.

4. Conclusions

We have investigated the surface and interface properties of six-period $Al_xGa_{1-x}N$/GaN SL grown by MOCVD on (0001) sapphire substrates. High-resolution XRD is used to

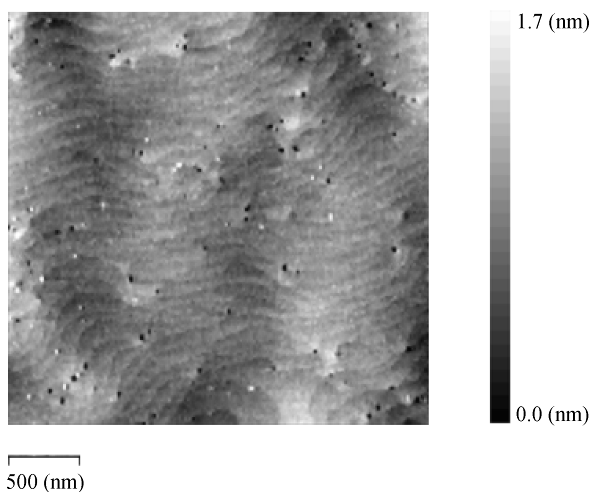

Fig. 5. AFM image of sample A, which shows remarkable step flow growth. The gray scale is 1.7 nm and the lateral dimensions are in μm. The RMS roughness values obtained from the GIXR and AFM techniques are 0.50 and 0.45 nm.

evaluate strains, layer thickness and composition in these structures. Application of the surface and interface sensitive GIXR technique has provided insight into the smoothness of these interfaces. The structure with a low Al mole fraction ($x = 0.25$) and thin well width has a rather smooth surface and interfaces while with high Al mole fraction ($x = 0.45$) has much rougher surface and interfaces. The surface roughness by GIXR was confirmed by AFM results. AFM images also showed the presence of atomic steps with large lateral dimensions, and the lateral step sizes larger than 100 nm exhibit smoother surfaces.

References

[1] Liu J, Zhou Y, Zhu J, et al. DC and RF characteristics of AlGaN/GaN/InGaN/GaN double-heterojunction HEMTs. IEEE Trans Electron Devices, 2007, 54: 2
[2] Adivarahan V, Gaevski M, Koudymov A, et al. Selectively doped high-power AlGaN/InGaN/GaN MOS-DHFET. IEEE Electron Device Lett, 2007, 28: 192
[3] Koudymov A, Shur M S, Simin G. Compact model of current collapse in heterostructure field-effect transistors. IEEE Electron Device Lett, 2007, 28: 332
[4] Ambacher O, Smart J, Shealy J R, et al. Two-dimensional electron gases induced by spontaneous and piezoelectric polarization charges in N- and Ga-face AlGaN/GaN heterostructures. J Appl Phys, 1999, 85: 3222
[5] Yu E T, Dang X Z, Asbeck P M, et al. Spontaneous and piezoelectric polarization effects in III–V nitride heterostructures. J Vac Sci Technol B, 1999, 17: 1742
[6] Smorchkova I P, Elsass C R, Ibbetson J P, et al. Polarization-induced charge and electron mobility in AlGaN/GaN heterostructures grown by plasma-assisted molecular-beam epitaxy. J Appl Phys, 1999, 86: 4520
[7] Zhang Y, Singh J. Charge control and mobility studies for an AlGaN/GaN high electron mobility transistor. J Appl Phys, 1999, 85: 587
[8] Maeda N, Tawara T, Saitoh T, et al. Doping design of GaN-based heterostructure field-effect transistors with high electron density for high-power applications. Physica Status Solidi A, 2003, 200: 168
[9] Kohn E, Daumiller I, Kunze M, et al. Transient characteristics of GaN-based heterostructure field-effect transistors. IEEE Trans Microw Theory Tech, 2003, 51: 634
[10] Kikuchi A, Bannai R, Kishino K, et al. AlN/GaN double-barrier resonant tunneling diodes grown by RF-plasma-assisted molecular-beam epitaxy. Appl Phys Lett, 2002, 81: 1729
[11] Lucas C A, Hatton P D, Bates S, et al. Characterization of nanometer-scale epitaxial structures by grazing-incidence X-ray diffraction and specular reflectivity. J Appl Phys, 1988, 63: 1936
[12] Fewster P F, Curling C J. Composition and lattice-mismatch measurement of thin semiconductor layers by X-ray diffraction. J Appl Phys, 1987, 62: 4154
[13] Takagi S. Dynamical theory of diffraction applicable to crystals with any kind of small distortion. Acta Crystallographica Section A: Foundations of Crystallography, 1962, 15: 1311
[14] Taupin D. Théorie dynamique de la diffraction des rayons X par les cristaux déformés. Bull Soc Fr Mineral Cristallogr, 1964, 87: 469
[15] Parrat L G. Surface studies of solids by total reflection of X-rays. Phys Rev, 1954, 95: 359
[16] Nevot L, Croce P. Surface characterization by grazing X-ray reflection—application to the study on some silicate glass polishing. Rev Phys Appl, 1980, 15: 761
[17] Wright A F. Elastic properties of zinc-blende and wurtzite AlN, GaN, and InN. J Appl Phys, 1997, 82: 2833